Appl Phys B (2011) 102: 95–100
DOI 10.1007/s00340-010-4210-8

Applied Physics B
Lasers and Optics

Experimental demonstration of near-field focusing of a phase micro-Fresnel zone plate (FZP) under linearly polarized illumination

R.G. Mote · S.F. Yu · A. Kumar · W. Zhou · X.F. Li

Received: 1 April 2010 / Revised version: 28 July 2010 / Published online: 25 September 2010

Abstract A high numerical aperture binary phase micro-Fresnel zone plate (FZP) is designed and fabricated on a glass substrate by using a focused ion beam technique. Focusing characteristics of the phase micro-FZP are measured by a near-field scanning optical microscope using linearly polarized light as an illumination source. It is found that an asymmetric spot with subwavelength beam width and elongated depth of focus can be obtained from the phase micro-FZP. Furthermore, the measurement is shown to be consistent with the calculation result. Further, the tolerance in fabrication errors like tilt of side walls on focusing is discussed with numerical simulations.

1 Introduction

Planar focusing devices based on near-field diffractive optics such as Fresnel zone plates (FZPs) may be a promising choice to realize compact optoelectronic systems such as CDs, DVDs and other optical data storage systems due to their ease of fabrication and integration with other optical elements. Furthermore, near-field diffractive optics operating in the visible spectrum can achieve resolution well below the optical resolution limits of Abbe and Rayleigh [1]. Despite their advantages in operating at visible wavelengths, FZPs were mainly used for X-ray microscopy and spectroscopy [2, 3]. This is because there is no suitable optical material that can be used to realize refractive optics at X-ray wavelengths. The poor light collection efficiency of FZPs has constrained their potential applications in compact optoelectronic systems. In far-field focusing, a FZP with a small number of zones may deteriorate the resolution due to increase in side lobes. However, the use of a compact FZP structure for near-field focusing (defined in this article as a micro-FZP) has been demonstrated [4–7]. Such a micro-FZP structure having subwavelength zones shows unique characteristics of suppression of higher diffraction orders, elongated focal length and subwavelength focal spot size [4]. Nevertheless, the possibility to achieve focusing in the near field from phase micro-FZPs has yet to be verified experimentally.

Under linearly polarized illumination, high numerical aperture (NA) focusing elements focus light into a rotationally asymmetric focal spot [8–10]. In our earlier work [5], we have discussed the asymmetry in the focusing with a high NA phase micro-FZP in the near-field focusing. It was shown that modulation of the etch depth in a phase micro-FZP improves the symmetry of a spot to a certain extent. Complete rotational symmetry is possible with the use of inherent symmetry in radially polarized illumination. The use of radial polarization is gaining interest due to promising results in applications like material processing [11], optical data storage [12], microscopy [13], optical trapping [14] and plasmonic focusing [15–17]. However, the use of a radially polarized source is limited by the need for more complicated optics [18].

R.G. Mote · W. Zhou
Precision Engineering & Nanotechnology Centre, School of Mechanical & Aerospace Engineering, Nanyang Technological University, Singapore 639798, Singapore

S.F. Yu (✉)
Department of Applied Physics, The Hong Kong Polytechnic University, Hung Hum, Kowloon, Hong Kong, China
e-mail: sfyu21@hotmail.com

A. Kumar · X.F. Li
School of Electrical & Electronic Engineering, Nanyang Technological University, Singapore 639798, Singapore

In this paper, near-field focusing of linearly polarized (LP) light by a large NA phase micro-FZP is demonstrated experimentally. We demonstrate, for the first time, fabrication of a binary phase micro-FZP with ultra-short focal length (i.e. a focal length shorter than the illumination wavelength) and optical characterization of such a high NA ($\rightarrow 1$) micro-FZP in the near field. Focused ion beam (FIB) technology is used to fabricate the phase micro-FZP on a glass substrate. The focusing characteristics of the phase micro-FZP are measured by a near-field scanning optical microscope (NSOM). It is found that the near-field focusing of LP light by the phase micro-FZP yields an asymmetric spot with a subwavelength beam width and an elongated depth of focus (DOF). In addition, the measured results are found to be consistent with the predictions from finite-difference time-domain (FDTD) simulations.

2 Design, fabrication and measurement of phase micro-FZP

The zone plate structure dimension can be estimated with a classical Fresnel zone plate equation:

$$r_n = \sqrt{n\lambda f + \frac{n^2\lambda^2}{4}}, \tag{1}$$

where r_n is the radius of the nth Fresnel zone, λ is an incident illumination wavelength and f is the focal length. We must emphasize that although the structure follows the classical equation used in far-field focusing, in the case of near-field focusing ($f \sim \lambda$) the presence of subwavelength zones suppresses higher diffraction orders making the focusing phenomenon different from the prediction of classical theory. Thus, dimensions obtained from (1) are for reference only and will be modified to optimize the focusing performance in the near-field regime.

A binary phase micro-FZP having eight full zones (i.e. 16 Fresnel zones) with a focal length of 500 nm under 633 nm wavelength illumination is considered in this investigation. To ease the fabrication process, an etch depth of 300 nm was used in this investigation because our previous studies have shown the possibility to use an etch depth of 300 nm to achieve near-field focusing [4]. The micro-FZP was realized on a glass substrate by using FIB technology (FEI quanta 200 3D dual-beam system). In order to minimize the charging effects during the fabrication, a layer of conductive ITO (~50 Ω/sq. inch) was coated on the glass substrate. To minimize redeposition of milled material, a parallel milling strategy has been employed to etch all the zones of the micro-FZP simultaneously. To achieve submicron features of the micro-FZP, the beam current was set at 30 pA with an accelerating voltage of 30 keV.

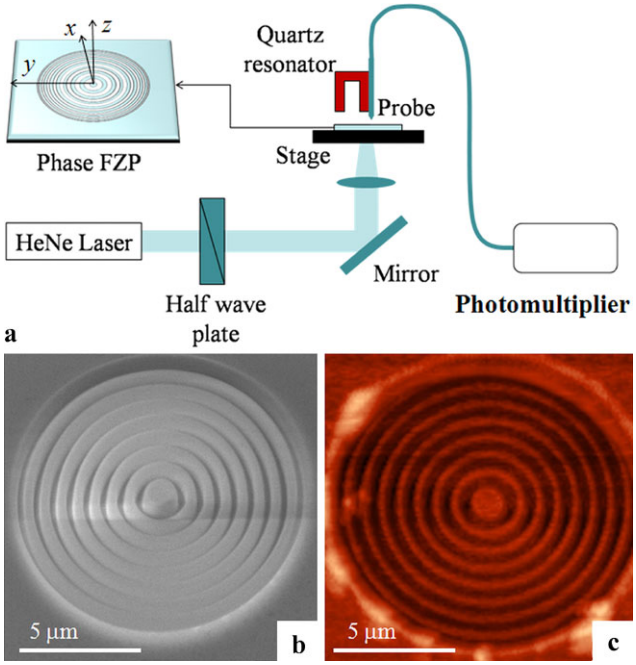

Fig. 1 (**a**) Near-field measurement set-up. Measured topography of a FIB fabricated binary phase micro-FZP. (**b**) SEM micrograph, (**c**) NSOM measurement. The phase micro-FZP has eight full zones and the corresponding etch depth is about 300 nm

Optical measurements were carried out by a NSOM (NTEGRA NT-MDT) operating in a collection mode (Fig. 1a). A LP helium–neon (632.8 nm) laser, whose polarization angle can be adjusted by a half-wave plate, was used as the illumination source. An Al-coated probe, which was glued to a quartz tuning fork, was employed to collect light emission from the surface of the phase micro-FZP. The probe has an average aperture diameter of 100 nm in order to ensure a subwavelength resolution of the system. Electric field intensity was mapped to the phase FZP by scanning the probe over its entire surface. A topographical signal and optical signals were collected simultaneously for all measurements. Figure 1b and c show a scanning electron microscope (SEM) micrograph and a topographical profile obtained from NSOM measurements of the phase micro-FZP, respectively. The etch depth of the micro-FZP is found to be about 300 nm.

3 Results

Figure 2a records the intensity pattern at $z \sim 10$ nm above the surface of the phase micro-FZP. It is noted that the intensity pattern is dominated by the interference of diffracted evanescent waves. No focusing is observed at this value of z.

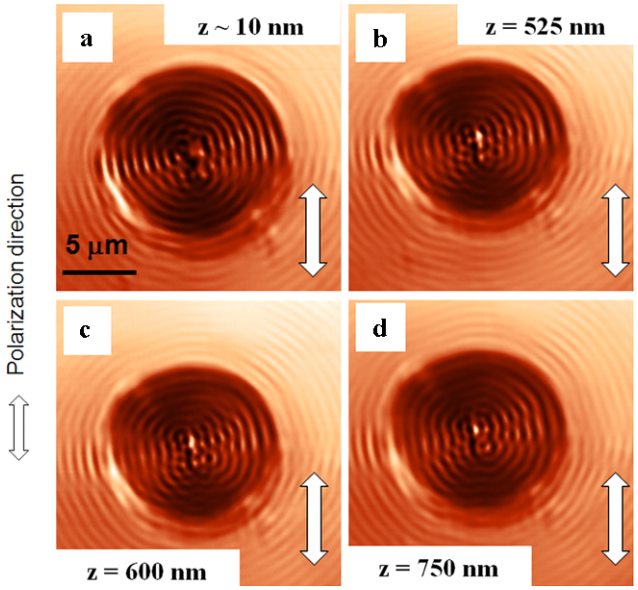

Fig. 2 Profiles of electric field intensity after being transmitted through a phase micro-FZP at planes located at (**a**) $z \sim 10$ nm, (**b**) $z = 525$ nm, (**c**) $z = 600$ nm and (**d**) $z = 750$ nm from the surface of the phase micro-FZP. The incident polarization is shown with a *solid white arrow*

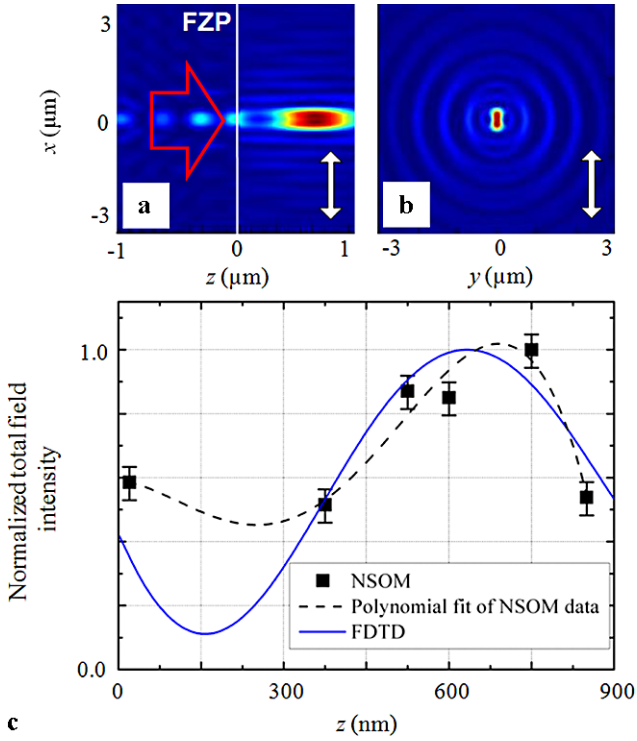

Fig. 3 Plot of normalized total electric field intensity, $|E|^2$, after being transmitted through a phase micro-FZP along (**a**) x–z plane and (**b**) the focal (x–y) plane located at $z = 630$ nm obtained from the FDTD simulation. The incident polarization is shown with a *solid white arrow*. (**c**) Comparison of total intensity obtained by FDTD results and NSOM measurements along propagation direction (z-axis). Error bar depicts fourth-order polynomial fit to NSOM data standard deviations (*upper error bars*) and measurement errors (*lower error bars*)

Figure 2b to d show the focusing characteristics of the illumination light at a distance z varying between 525 and 750 nm from the surface of the phase micro-FZP. It is observed that all the focal spots have a rotationally asymmetric profile. Focal spots are broadened along the x-axis (i.e. polarization direction) when compared to that along the y-axis. This is because the phase micro-FZP bears a high numerical aperture (NA = 0.99). When a high NA focusing system is illuminated by LP light, the vectorial nature of the light makes resolutions substantially different in the plane of polarization [9, 10].

Focusing behavior of the phase micro-FZP is also analyzed by using a complete vectorial FDTD simulation (FDTD Solutions, Lumerical Inc., Canada). In the simulations, the etch depth of the FZP was set at 300 nm. Figure 3a and b give the calculated total intensity profile of the focusing beam in the x–z (at $y = 0$ nm) and x–y (at $z = 630$ nm) planes, respectively. It is observed that the focusing beam has an asymmetric profile and is broadened along the polarization direction similar to that observed from the experimental results. Figure 3c compares the electric field intensity obtained from FDTD simulation and NSOM measurements along the propagation direction (i.e. z-axis). The experimentally observed focal length is about 700 nm and is close to that obtained from the FDTD calculation (i.e. 630 nm). The focal spot size at FWHM is found to be 520 and 225 nm along the x-axis (polarization direction) and the y-axis, respectively. On the other hand, highly intense focusing is seen over a distance of 250 nm (i.e. from $z = 500$ to 750 nm) along the z-direction. Such an elongated DOF is also in agreement with FDTD calculations.

Figure 4a and b shows measured focal field profiles at a distance z equal to 600 and 750 nm respectively from the surface of the phase micro-FZP. The spot size (FWHM) is measured to be about 600 and 400 nm along the x- and y-axes, respectively, in the plane of maximum intensity (i.e. $z = 750$ nm), see Fig. 4b. As the illumination light has a wavelength of 632.8 nm, it is verified that the phase micro-FZP can achieve subwavelength focusing of the light beam. It is also observed from the figures that the focal spots along the y-axis are accompanied by high-intensity side lobes. As the focal spot along the y-axis is tighter than that along the x-axis, the intensities of the side lobes must increase due to the principle of energy conservation. Such high-intensity side lobes have been predicted during tighter focusing with the aid of aperture plates [19, 20] and often deteriorate the resolution. However, the intensity of side lobes obtained from the measurement is found to be higher than that obtained from the FDTD calculation.

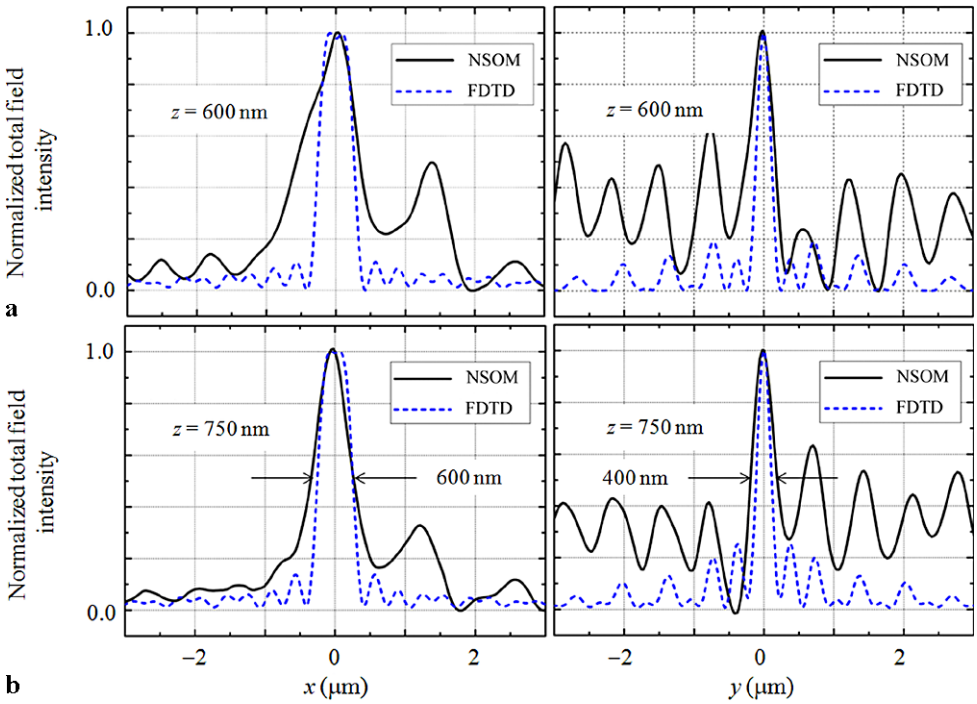

Fig. 4 Plot of normalized total electric field intensity, $|E|^2$, after passing through a phase micro-FZP in the x–y plane obtained from the NSOM measurement (*solid lines*) and FDTD simulation (*dashed lines*). (**a**) $z = 600$ nm and (**b**) $z = 750$ nm

4 Discussion

The excitation of side lobes can be attributed to the poor diffraction efficiency of the zones of the phase micro-FZP. This is mainly due to the FIB fabrication process induced structural damage to the phase micro-FZP [21]. Optical properties of the target material such as refractive index may be altered by Ga^+-ion-beam bombardment [22]. Moreover, such an index change is not uniform across all the zones of the phase micro-FZP as each zone is exposed to a different ion dose due to the different zone width during the FIB etching process. As a result, index variations over the phase micro-FZP can change the phase retardation of the individual zones of the micro-FZP leading to an inefficient diffraction. Another issue arising from the use of FIB to fabricate the phase micro-FZP is that the FIB milled trenches deviate from the designed vertical side walls and the resulting shape is similar to a 'V' [23, 24]. Figure 5 shows a SEM sectional view of the micro-FZP structure fabricated under a similar condition as discussed earlier. Platinum was deposited at a beam current of 0.1 nA over the region to be sectioned in order to protect the structure during sectioning and to improve the contrast during imaging. Side wall tilts are found to be less than 20° and the designed zone width is maintained at the center. Tilted side walls cause phase retardation introduced by an etch depth not in congruence with the design value and thus causing deviation from the predicted focusing performance. Another source of errors may be associated with the NSOM measurement. The coupling of the electric field through the probe may change the value of the true field and thus introduce errors in the measurement. In addition, as NSOM probes may not exhibit equal sensitivity to all field components, the total intensity measured may deviate from the actual intensity value [25]. In addition, misalignments in the optical measurement devices also contribute to the total error.

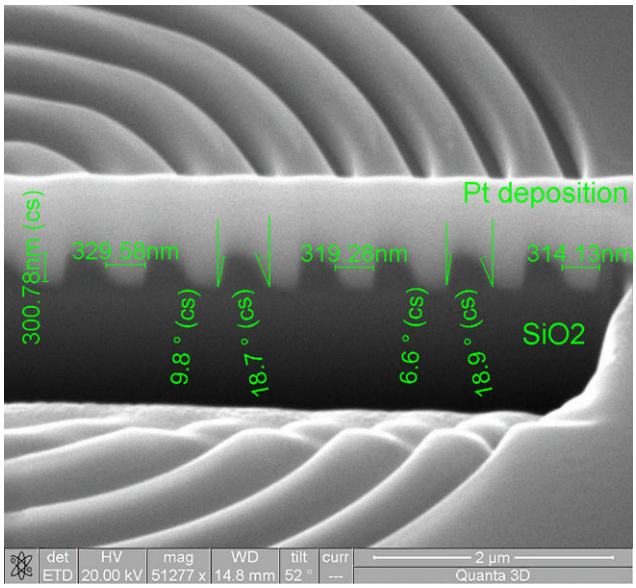

Fig. 5 SEM image of FIB sectioned phase micro-FZP with focal length 0.5 μm

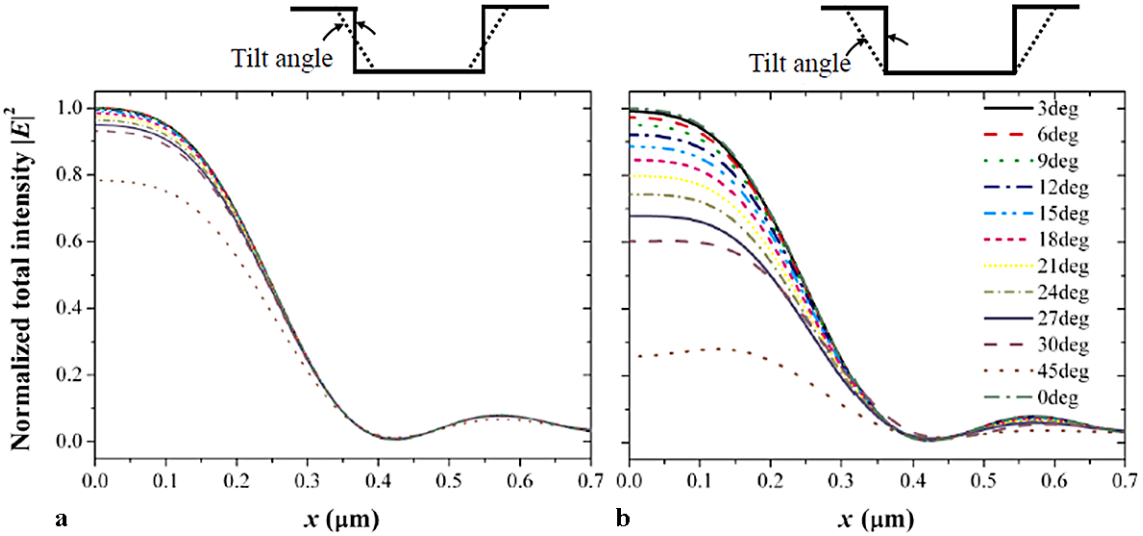

Fig. 6 Influence of zone wall tilt on focusing intensity ($|E|^2$) of phase micro-FZP calculated by FDTD simulations. The designed zone width is at (**a**) center and (**b**) bottom of groove. Intensities are normalized by electric field intensity calculated with vertical side walls (i.e. tilt angle = 0). The phase micro-FZP has a focal length of 0.5 μm ($\lambda = 633$ nm)

5 Influence of tilt of side walls on focusing performance

For the case of a phase micro-FZP with 500 nm focal length, we have studied the influence of non-vertical side walls on focusing characteristics with FDTD simulations. In order to represent tilted side walls, a refined mesh of $8 \times 8 \times 8$ nm^3 is used in the micro-FZP region and $15 \times 15 \times 15$ nm^3 elsewhere. In order to minimize memory requirements, a 200 nm etch depth is used for simulations. Tilt of side walls is considered in two configurations: the designed zone width is maintained at (1) center and at (2) base of the zone depth as shown in Fig. 6. The design is found to be more tolerant to the side wall tilts if the designed zone width is maintained at the center because phase errors introduced are compensated due to the complementary nature of tilts above and below the center line. The focusing intensity is reduced by 20% when the tilt angle is 45°. However, with the other configuration, the intensity reduces by 75%. This may be attributed to the increase of diffractive scattering losses as the zone width is broadened across the zone height.

6 Conclusions

In conclusion, a binary phase micro-FZP has been fabricated on a glass substrate by using FIB to achieve near-field focusing in the visible spectrum. NSOM measurements revealed rotational asymmetry of a spot with subwavelength beam width due to high NA of the phase micro-FZP under LP illumination. In addition, the phase micro-FZP has demonstrated an elongated DOF (∼250 nm), which may be used to realize an auto-focusing feature in optical systems. The experimental results verify the subwavelength focusing as obtained from the FDTD simulation. The influence of tilted side walls due to fabrication errors is studied through FDTD simulation and the extent to which tilt can be tolerated is determined. Furthermore, the proposed phase micro-FZP has the advantages of (1) simplicity of fabrication due to the use of a single material planar structure and (2) high diffraction efficiency due to the phase nature of its focusing mechanism. Therefore, it may find useful applications in many near-field operating systems such as near-field imaging and sensing as well as optical data storage.

Acknowledgements This work is supported by the A*STAR SERC grant no. 082-101-0016. The FIB system used in the work was supported under the A*STAR SERC grant no. 072-101-0023.

References

1. D. Marks, P.S. Carney, Opt. Lett. **30**, 1870 (2005)
2. W. Chao, B.D. Harteneck, J.A. Liddle, E.H. Anderson, D.T. Attwood, Nature **435**, 1210 (2005)
3. M. Peuker, Appl. Phys. Lett. **78**, 2208 (2001)
4. R.G. Mote, S.F. Yu, B.K. Ng, W. Zhou, S.P. Lau, Opt. Express **16**, 9554 (2008)
5. R.G. Mote, S.F. Yu, W. Zhou, X.F. Li, Appl. Phys. Lett. **95**, 191113 (2009)
6. L. Feng, K.A. Tetz, B. Slutsky, V. Lomakin, Y. Fainman, Appl. Phys. Lett. **91**, 081101 (2007)
7. H.C. Kim, H. Ko, M. Cheng, J. Vac. Sci. Technol. B **26**, 2197 (2008)
8. E. Wolf, Proc. R. Soc. A **253**, 349 (1959)
9. B. Richards, E. Wolf, Proc. R. Soc. A **253**, 358 (1959)
10. R. Dorn, S. Quabis, G. Leuchs, J. Mod. Opt. **50**, 1917 (2003)
11. A.V. Nesterov, V.G. Niziev, J. Phys. D **33**, 1817 (2000)

12. K. Wan-Chin, P. No-Cheol, Y. Yong-Joong, C. Hyun, P. Young-Pil, Opt. Rev. **14**, 236 (2007)
13. Y. Shuangyang, Z. Qiwen, J. Opt. A **10**, 125103 (2008)
14. Z. Qiwen, Opt. Express **12**, 3377 (2004)
15. J. Wang, W. Zhou, A.K. Asundi, Opt. Express **17**, 8137 (2009)
16. A. Yanai, U. Levy, Opt. Express **17**, 924 (2009)
17. F.I. Baida, A. Belkhir, Plasmonics **4**, 51 (2009)
18. Q. Zhan, Adv. Opt. Photon **1**, 1 (2009)
19. H. Liu, Y. Yan, D. Yi, G. Jin, Appl. Opt. **42**, 1463 (2003)
20. T.R.M. Sales, G.M. Morris, J. Opt. Soc. Am. A **14**, 1637 (1997)
21. B. Basnar, A. Lugstein, H. Wanzenboeck, H. Langfischer, E. Bertagnolli, E. Gornik, J. Vac. Sci. Technol. B **21**, 927 (2003)
22. Y.Q. Fu, N.K.A. Bryan, Appl. Phys. B **80**, 581 (2005)
23. Y.Q. Fu, W. Zhou, L.E.N. Lim, C. Du, H. Shi, C.T. Wang, X. Luo, J. Comput. Theor. Nanosci. **4**, 614 (2007)
24. Y.Q. Fu, W. Zhou, L.E.N. Lim, C. Du, H. Shi, C.T. Wang, X. Luo, Appl. Phys. B **86**, 461 (2007)
25. G.M. Lerman, A. Yanai, U. Levy, Nano Lett. **9**, 2139 (2009)